Journal of Sensor Technology, 2024, 14, 51-67
https://www.scirp.org/journal/jst
ISSN Online: 2161-1238
ISSN Print: 2161-122X

Impedimetric Sensor of Lanthanum and Cerium Ions Based on Functional Isosorbide-Based Oligo (Ether Sulfone) S-Modified Platinum Electrodes

Marwa Sebai[1], Nour El Houda Brirmi[1], Taha Chabbah[2], Saber Chatti[1], Kamel Alimi[3,4], Regis Mercier[2], Catherine Marestin[2], Hamdi Ben Halima[5], Boris Lakard[5], Nicole Jaffrezic-Renault[5]*

[1]Laboratory of Natural Substances, National Institute of Research and Physicochemical Analysis (INRAP), Biotechnopole of Sidi Thabet, Ariana, Tunisia
[2]Institute of Polymer Materials IMP-INSA, University of Lyon, Villeurbanne, France
[3]Analytical Platform, National Institute of Research and Physicochemical Analysis (INRAP), Biotechnopole of Sidi Thabet, Ariana, Tunisia
[4]Research Laboratory Number 18ES19, University of Monastir, Monastir, Tunisia
[5]Joint Research Unit Number 6213, UTINAM Institute, University of Franche-Comte, Besançon, France
Email: *njaffrezic@gmail.com

How to cite this paper: Sebai, M., Brirmi, N.E.H., Chabbah, T., Chatti, S., Alimi, K., Mercier, R., Marestin, C., Halima, H.B., Lakard, B. and Jaffrezic-Renault, N. (2024) Impedimetric Sensor of Lanthanum and Cerium Ions Based on Functional Isosorbide-Based Oligo (Ether Sulfone) S-Modified Platinum Electrodes. *Journal of Sensor Technology*, **14**, 51-67.
https://doi.org/10.4236/jst.2024.144004

Received: August 30, 2024
Accepted: October 7, 2024
Published: October 10, 2024

Abstract

Rare earth elements (REEs) are beneficial in developing modern technologies, especially electronics. Their extractions from natural deposits and their recycling require chemical processes that should be monitored regarding efficiency and environmental sustainability. The purpose of this study is to develop impedimetric sensors for the sensitive detection of the rare earth elements La and Ce by modifying a platinum electrode with four isosorbide-based oligo (ether sulfone)s. These oligomers, functionalized with different end groups (hydroxyl, fluor, amine, maleimide), were obtained with satisfactory yields, starting from isosorbide and bis (4-fuorophenyl) sulphone monomers. The resulting oligomers were characterized by NMR, DSC, and ATG analysis. The dihydroxy-oligo (ether sulfone) modified sensor showed the highest analytical performance compared to the other oligomers. The detection limit is 10^{-9} M for La and 3×10^{-9} M for Ce which is lower than that of most of the published electrochemical sensors.

Keywords

Rare-Earth Elements, Dihydroxy-Oligo (Ether Sulfone) Modified Platinum Electrode

1. Introduction

Nowadays, rare earth elements (REEs) provide essential components in numerous fields of industry for their optical, magnetic, and mechanical properties [1]. These elements are used in the permanent magnets of wind turbines and hard disks, petroleum catalysis, polishing, alloys and glass manufacturing, and rechargeable vehicle batteries. Their applications range from heavy industry to consumer products. An analysis of supply and demand for each REEs revealed that in 2020, global world demand was around 200,000 tonnes per year. Considering the significant increase in global demand, ensuring the continued availability of these elements is a major challenge for the ecological and digital transition. Nevertheless, the risk associated with the production of heavy and light rare earth elements remains significant, as the European Commission classifies them as critical raw materials [2]. Besides this economic and geopolitical observation, rare earth elements are often extracted under environmental conditions that still need to be optimised [3] [4].

Several techniques have been used to detect REEs, such as X-ray fluorescence spectrometry (XRF) [5], inductively coupled plasma mass spectroscopy (ICP-MS) [6], mass spectrometry [7]-[9], electrophoresis method combined with non-contact capacitively coupled conductivity detection (C4D) [10], high-frequency non-contact conductivity detector [11]-[15], activation analysis [16]. However, these laboratory techniques are generally complex and require expensive equipment and specific skills for reliable analysis. Therefore, electrochemical sensors based on portable instrumentation appear to be very attractive devices for detecting REEs, thanks to their usual intrinsic characteristics (high sensitivity, detection limit in the range of nM or less, short analysis time, and low cost). Potentiometric and voltammetric sensors [17] were designed to detect some rare earth elements.

To make the detection process eco-friendly, it was proposed to use a biobased polymer as a modifier of the electrodes for the sensitive impedimetric detection of cerium (Ce) and lanthanum (La) ions, the most abundant rare earth elements in the earth's crust. Functionalized polyethersulfone was used as a modifier for GCE in the sensitive voltammetric detection of yttrium [18]. Four isosorbide-based oligo (ethersulfone)s were synthesised. Isosorbide improves the mechanical properties of the obtained polymer and it presents UV resistance, due to its unique molecular structure [19]-[21]. The non-toxicity of isosorbide was proven; it was widely used in pharmaceutical and cosmetic products [22] [23]. Isosorbide generates the hydrophilicity and wettability of the resulting linear polymer, which regulates the availability of adsorption sites and the dispersion of the polymer in water. For these reasons, the isosorbide-based poly (ether sulfone) constitute an important class of specialised thermoplastic polymers [24]-[26]. It is distinguished by a high glass transition temperature (190˚C), an amorphous transparency, high hydrolytic stability, and a low sensitivity to oxidation. It can then be used at high process temperatures (220˚C - 250˚C). In this study, a series of oligo (ether sulfones), distinguished by the functional moiety at the extremity of their chains, were designed. The obtained oligomers were fully characterized using RMN spectroscopy, DSC, and ATG, and the analytical performance of the modified electrodes for the detection of La and Ce was then determined using electrochemical impedance spectroscopy.

2. Experimental

2.1. Reagents and Standards

N,N-dimethylformamide (DMF) (≥99.9%) was purchased from Sacharlab. 1,4:3,6-dianhydro-d-glucitol (isosorbide) (IS) (≥99.9%) and bis(4-fluorophenyl) sulfone (DFDPS) (≥99.0%) were both purchased from Acros Organics. IS was employed after recrystallisation in acetone and dried over P_4O_{10} in a desiccator. Acetic anhydride (AAn) (≥99.0%), 3-aminophenol (≥98.0%), maleic anhydride (MAn) (≥99. 0%), anhydrous potassium carbonate (K_2CO_3) (≥99.7%), anhydrous sodium acetate (NaOAC) (≥99.0%) and methanol (MeOH) (≥99.9%) were procured by Sigma Aldrich. These products were used as described. The REEs studied here, Cerium (Ce) and Lanthanum (La), were used without further purification.

2.2. Characterization Methods

The 300 MHz NMR spectra were recorded on a Bruker Advance spectrometer in 5 mm i.d. sample glass tubes using DMSO-d6 as solvent.

To obtain oligomer masses of 3000 g/mol, calculations of several polycondensation parameters were carried out using the following equations eq 1 and eq 2.

$$M_n = M_0 \times X_n + M_{\text{ext}} \qquad \text{(eq 1)}$$

with M_n = the number average molecular weight of oligomer;

M_0 = the molecular mass of repeating unit;

M_{ext}= the molecular mass of end-groups;

X_n = DP= Degrees of polymerization (the number of repeat units n).

Then, using the expression

$$X_n = (1+r)/(1+r-2rp) \qquad \text{(eq 2)}$$

with r = stoichiometric ratio, p= degrees of advancement assuming 1 we can calculate the stoichiometric ratio $r = (X_n - 1)/(X_n + 1) = 0.777$. Finally, we set the number of moles of excess monomer, to calculate the number of moles of default monomer by the relationship $r = n(\text{default reagent})/n(\text{excess reagent})$.

A thermogravimetric analysis (TGA) was conducted using a TA Instruments TGA Q50 in a temperature range of 25˚C - 600˚C under nitrogen at a heating rate of 10˚C/min. Glass-transition temperatures (Tg) of the oligomers were determined using a Mettler-Toledo DSC822e differential scanning calorimeter at a heating rate of 10˚C/min under nitrogen atmosphere.

2.3. Oligo (Ether Sulfone) Synthesis

As illustrated in **Figure 1**, a series of four oligo (ether sulfone)s with different end-groups (F, OH, NH_2 and maleimide) were prepared according to our published article [27].

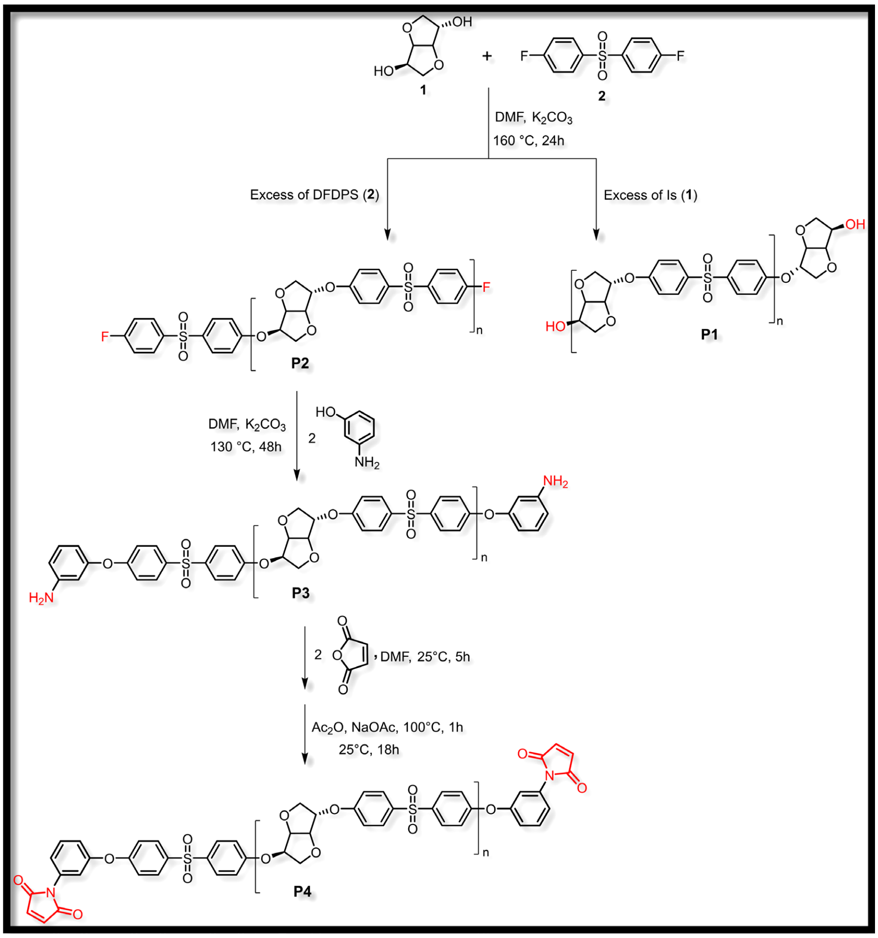

Figure 1. Synthesis of isosorbide-based olig(ether sulfone)s with different end-groups (OH, F, NH_2 and maleimide) P1-P4 (M_n = 3000 g/mol, n = 8).

2.3.1. Synthesis of Dihydroxy-Oligo (Ether Sulfone) (P1)

The polycondensation was performed by reacting 20.0 mmol of IS (1), 15.4 mmol of DFDPS (2), and 44 mmol of K_2CO_3 in 50 mL of DMF, into a 250-mL cylindrical two-neck glass reactor, equipped with a mechanical stirrer. 20 mL of toluene was dropwise added through a dropping funnel. The reaction mixture was heated until 140˚C so that a slow azeotropic distillation of the toluene was observable. The loss of toluene was replaced continuously by the dropping funnel. The temperature was then slowly increased to 160˚C for 24 h. The hydroxy end-group was controlled by ^1H NMR spectroscopy. Finally, the obtained viscous solution was precipitated into methanol. The precipitate was collected by filtration, washed thoroughly with cold methanol, and then dried in a vacuum. The oligomer P1 was isolated as a white powder with a 95% yield.

2.3.2. Synthesis of Difluoro-Oligo (Ether Sulfone) (P2)

In a two-necked reactor equipped with a N_2 inlet and a mechanical stirrer, a mixture of 15.4 mmol of IS (1), 20.0 mmol of DFDPS (2), 33.88 mmol of K_2CO_3 and 50 mL of DMF was stirred and heated at 160˚C for 24 h. The fluoro end-group was controlled by proton NMR spectroscopy. The solution was then poured into methanol, filtrated and washed with methanol. After drying under vacuum, a white crystal was obtained with a 96% yield.

2.3.3. Synthesis of Diamine-Oligo (Ether Sulfone) (P3)

In a 100 mL two round-bottom flask equipped with N_2 inlet, 4 g of the resulting di-fluorinated oligomer P2, 0.60 g of 3-aminophenol and 4.00 mmol of K_2CO_3 were dissolved in 20 mL of DMF. The mixture was then stirred for 48 h at 130˚C. The reaction solution was poured into methanol, filtered, and dried under vacuum at 40˚C, giving a brown powder with a yield of 87%.

2.3.4. Synthesis of Bismaleimide-Oligo (Ether Sulfone) (P4)

A 100-mL two-necked, round-bottomed flask equipped with a magnetic stirrer bar, a nitrogen-gas inlet tube, and a calcium chloride drying tube, was charged with 1.80 g of resulting diamine P3, 115.0 mg of maleic anhydride (MAn) and 10 mL of DMF. The mixture was stirred at room temperature for 5 h. The formed bismaleamic acid was then converted into bismaleimide via a chemical-imidization process. The amide acid cyclization was carried out by adding 0.3 mL of acetic anhydride and 20 mg of anhydrous sodium acetate to the intermediate solution, while stirring it at 100˚C for 1 h. The mixture was then stirred overnight at room temperature. Finally, the oligomer solution was slowly poured into methanol to form a precipitate. The precipitate was then filtered, washed thoroughly with methanol, and dried overnight under a vacuum at 80˚C, a yield of 85% was obtained.

2.4. Electrochemical Characterization

EIS measurements were carried out using a SP-200 potentiostat (Biologic) using EC-Lab V11.43 software. This device generates the sinusoidal signal with the desired amplitude and frequency and recovers the real and imaginary parts of the impedance system under study. In these tests, the initial potential was $E = -0.15$ V, the frequency range was set from 1 kHz to 100 mHz, and an amplitude of 10 mV superimposed on the DC voltage. All measurements were performed in an identical solution and at room temperature to minimize the variations of resistance. Real and imaginary impedances were calculated and a Nyquist diagram was traced. The impedance values were adjusted using Scribner Associates "Zview" software.

The electrochemical measurements were performed in a Pyrex glass cell using a polymer-coated platinum electrode as the working electrode, an Ag/AgCl reference electrode, and an auxiliary platinum electrode (99% purity), used to close the electrical circuit in the electrochemical cell. For each measurement, the position of the electrodes remained the same. The electrochemical cell was placed in a Faraday cage to reduce the influence of electromagnetic waves. All measurements were performed with the polymer-modified platinum electrode immersed in a 0.2

M potassium citrate solution (pH 4.0) containing the rare earth ions after 25 min of equilibration.

2.5. Preparation of Polymer-Modified Platinum Electrodes

Platinum electrodes were 1.2 × 1.2 cm square plates. The surface was rinsed with ethanol for 10 min, rinsed with ultrapure water, and then dried under flowing nitrogen. 5 µL of 1 w/w% dimethylsulfoxyde solution of P1, P2, P3 and P4 polymer were mixed separately and drop-casted on the electrode surface and then dried under nitrogen flow for 48 h, at room temperature.

3. Results and Discussion

3.1. Synthesis and Characterization of Oligo (Ether Sulfone)s P1 - P4

The dihydroxy and difluoro-ether sulfone oligomers P1 and P2 were prepared with a molecular ratio calculation of isosorbide (Is) and 4,4’-difluorodiphenylsulfone (DFDPS) monomers to get a M_n of 3000 g/mol. The monomer polycondensation was performed in DMF in the presence of potassium carbonate at 160˚C, as reported previously in the literature [27]. The condensation reactions were monitored by ^{1}H NMR spectroscopy to obtain the desired hydroxylated and fluorinated oligomers in satisfactory yields and almost quantitative functionalization. The oligoethersulfones P1 and P2 were isolated as a white powder after precipitation in methanol and dried under vacuum.

The repeat unit molecular weight (M_0) of each oligomer was equal to 361.07 g/mol, and the molecular mass of end groups was 146.06 g/mol and 254.02 g/mol for P1 and P2, respectively. Since the average molecular weight (M_n) of both target oligoethersulfones P1 and P2 was fixed at 3000 g/mol, the number of repeating units n in their principal chains, was found to be around 8.

The chemical structures of these oligoethersulfones were characterized by ^{1}H NMR. The proton NMR spectra of (OH)-oligomer P1, presented in **Figure 2**, exhibit the characteristic protons of isosorbide diol (H1 - H6) and DFDPS (H7 - H8). Moreover, the spectrum reveals the presence of low-intensity peaks corresponding to protons at the end groups of isosorbide (H1* - H6*) confirming the formation of hydroxyl-terminated oligomer. The proton NMR spectra of oligomer P2 clearly show the total protons characteristic of the repetitive unit with the presence of low-intensity peaks in the aromatic zone (H7* and H8*).

Fluorine atoms at oligomer P2 chain ends were successfully substituted with 3-aminophenol in the presence of K_2CO_3 in DMF at 130˚C for 48 h to afford the diamine-oligoethersulfone P3 (**Figure 1**). The nucleophilic displacement reaction of F-atoms by OH-PhNH$_2$ was confirmed by the appearance of the characteristic signal of amine protons H9 located in ^{1}H NMR spectra at 5.30 ppm (**Figure 2**), as well as the disappearance of the fluorine chain ends signals.

Oligomer containing maleimides end-groups P4 was finally synthesized with a good yield of 85%, according to a two-step procedure, which includes the condensation of the diamine P3 with maleic anhydride followed by the maleamic acid cyclization, as outlined in **Figure 1**. The first reaction was performed at room temperature in DMF. This fast and exothermic reaction leads to the intermediate bismaleamic acid. The chemical imidization process was then performed with acetic anhydride and a basic catalyst like sodium acetate giving the bismaleimide P4. The ^{1}H NMR spectrum of the representative oligomer (**Figure 2**), presents the total protons related to bismaleimide groups (H14 - H19) at the end of chains which are consistent with the proposed chemical structure for this oligomer.

The solubility of the resulting oligo (ether sulfone)s was tested by dissolving 10 mg of oligomers in 10 ml of solvent; in the case of insolubility, we assayed 1 mg in 1 ml of solvent. The results are summarized in **Table 1**. All the obtained oligomers (P1 - P4) exhibited excellent solubility in aprotic polar solvents such as DMSO, DMF, and NMP. They are insoluble in heptane, methanol, ethyl acetate, diethyl ether, acetonitrile and water, and partially soluble in acetone and THF, in particular for the P4 oligomer, which is soluble.

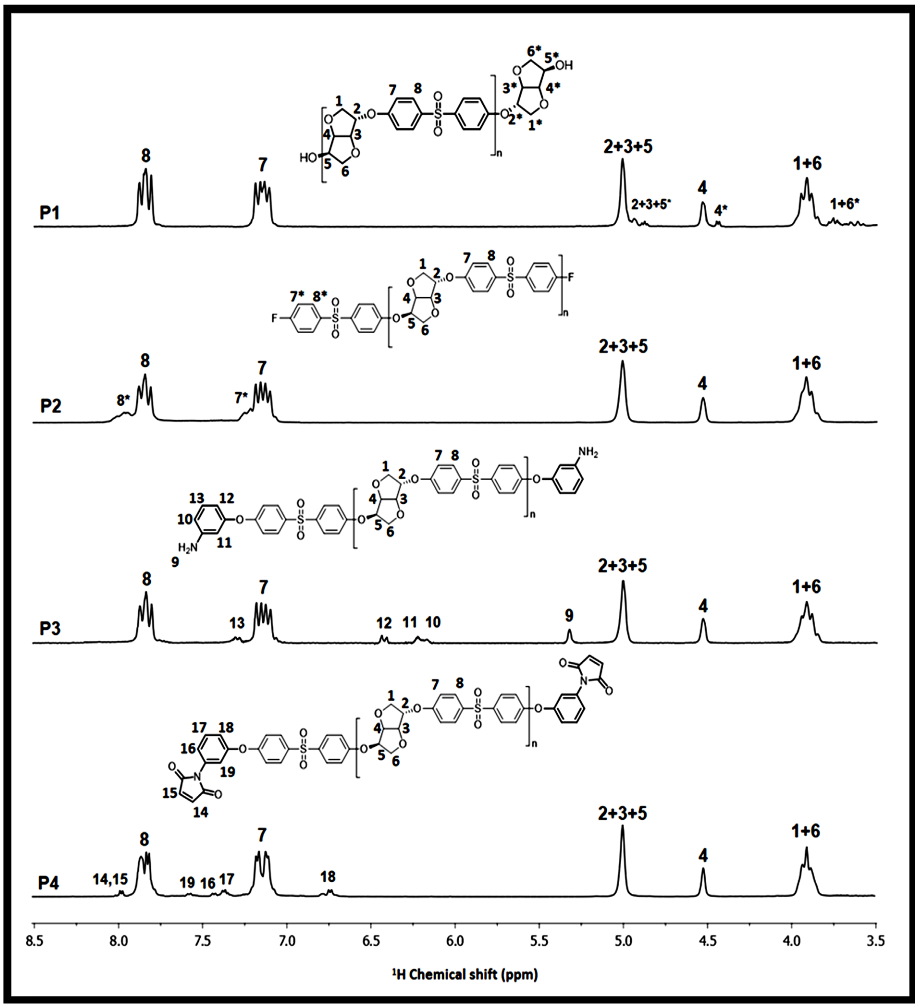

Figure 2. ^{1}H NMR spectra of Oligomers P1, P2, P3 and P4 in DMSO-*d*6.

Table 1. Solubility of oligomers.

	Solvents[a]											
N˚	$n\text{C}_7\text{H}_{16}$	MeOH	EtOAc	Et_2O	Acetone	THF	CH_2Cl_2	CHCl_3	CH_3CN	DMSO	NMP	H_2O
P1	–	–	–	–	~	~	~	+	–	+	+	–
P2	–	–	–	–	~	~	–	~	–	+	+	–
P3	–	–	–	–	~	~	~	+	–	+	+	–
P4	–	–	–	–	~	+	+	+	–	+	+	–

3.2. Thermal Properties of Oligomers

The thermal properties of functional oligo (ether sulfone)s P1-P4 were determined by Thermogravimetric analysis (TGA) and Differential Scanning Calorimetry (DSC). DSC analysis revealed the amorphous behaviour of the oligomers with high glass transition temperature values (T_g) ranging from 160 to 176˚C, depending on the nature of the functional group at the end of oligomer chains. The T_g values of diamine and dihydroxyoligoethersulfones (P3, 176˚C) and (P1, 171˚C) are higher than the T_g of difluoro-oligomer (P2, 160˚C) (**Table 2**). This result can be explained by the formation of inter- and intra-chain hydrogen bonds in P1 and P3 oligomers, leading to a decrease in chain mobility and flexibility with an increase in structural rigidity and glass transition temperature (T_g) [28].

The TGA experiments (**Table 2**) shows that all oligo (ether sulfone)s P1-P4 were thermally stable with decomposition temperatures for 5% weight losses (T_{d5}) higher than 300˚C, depending on the structure of the polymers. The highest thermal stability is observed for bismaleimide oligomer (P4) with a structure rich in aromatic rings (Td5 = 447˚C).

Table 2. Thermal properties of the resulting oligomers P1 - P4.

Oligomer	Chain end functions	Yield$^{a)}$ (%)	$T_g$$^{b)}$ (˚C)	$T_{d5}$$^{c)}$ (˚C)
P1	OH	95	171	321
P2	F	96	160	338
P3	NH_2	87	176	354
P4	maleimide	85	-	447

$^{a)}$ After precipitation into MeOH. $^{b)}$ Determined by DSC under nitrogen at a heating rate of 10˚C/min. $^{c)}$ Temperature at 5 wt % loss.

3.3. EIS Measurements for Detecting La

The impedance spectra of platinum electrode/oligo (ether sulfone)s/electrolyte obtained in the presence of increasing concentrations of La ions in an acetate solution are shown on the Nyquist plot in **Figure 3**, as solid points. An equivalent circuit modeled the electrical properties: Nyquist diagrams were compared with several electrical circuit models through Z-View software until the experimental data were fitted satisfactorily. The chosen model must fit the data with good precision and should not contain too many components. In our experiment, each spectrum shows the typical behavior of a semicircle associated with an equivalent circuit consisting of a resistor, R, in parallel with a constant phase element, CPE (**Figure 4**). As the concentration of lanthanum increases, the diameter of the semicircles decreases. The right-hand (low-frequency) end of a semicircle corresponds to the value of the resistor. The values of the equivalent electrical circuit's elements were obtained, corresponding to a correlation coefficient χ^2 equal to 10^{-3}. A higher concentration of La ions decreases the polarization resistance, which generates a lower impedance. This result can be explained by the adsorption of La ions on the oligo (ether sulfone)s.

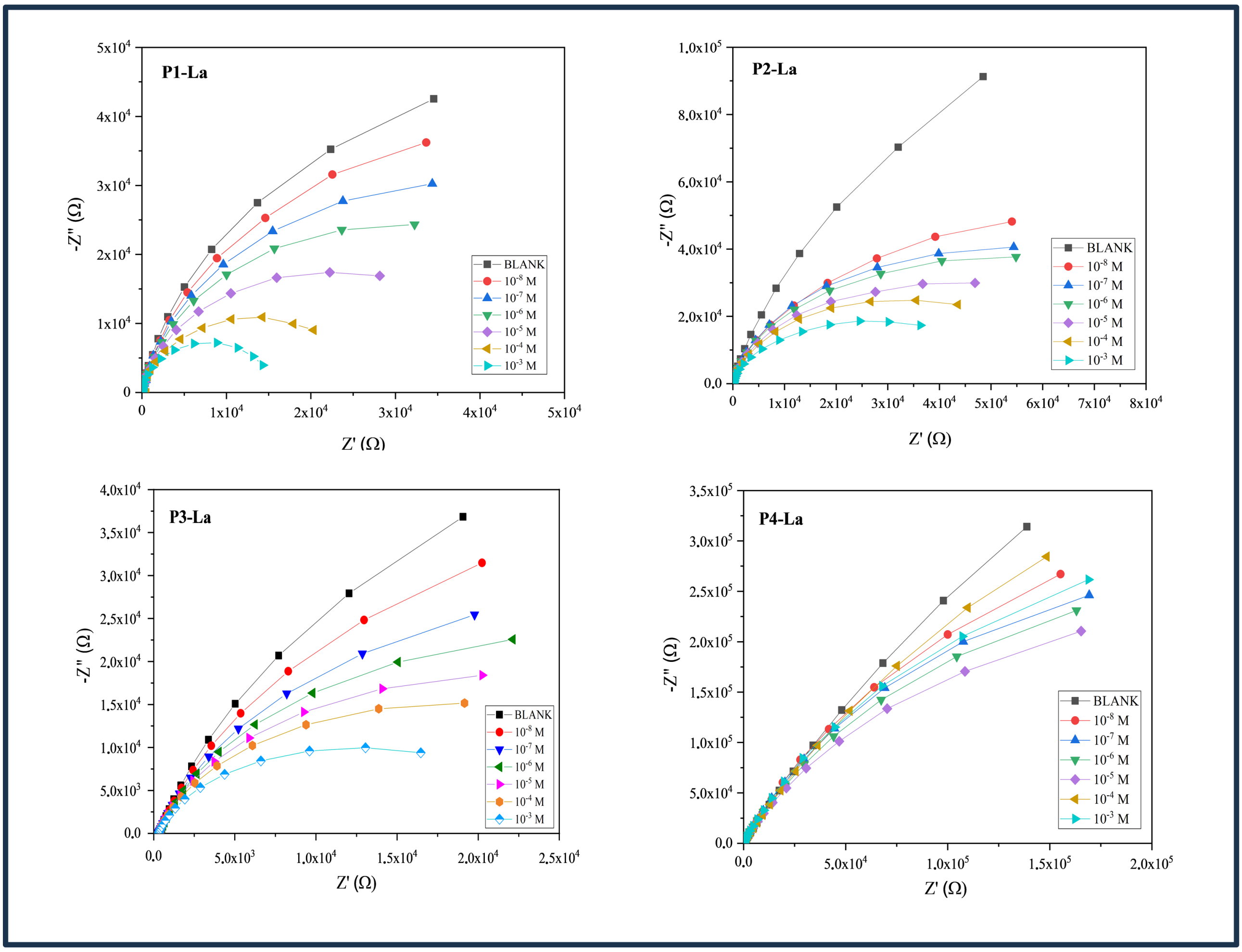

Figure 3. Nyquist plots of Pt/oligomer/electrolyte interface obtained in the presence of La ions.

The calibration curve of the sensor was obtained by plotting the relative variation of the charge transfer resistance of each platinum electrode modified with P1, P2, P3, and P4 oligomer respectively as a function of the logarithmic concentration of

La ion using the following equation: $\left|Rp0 - Rp\right| / Rp0\left(\Delta R/R\right)$. This parameter was found to be linearly proportional to the logarithmic value of La concentrations (pM) (**Figure 5**). To ascertain the limits of detection (LOD) and quantification (LOQ), the formulas Equation (3) and Equation (4), respectively, were used.

$$\text{LOD} = \frac{3 \times \text{Standard deviation of the intercept}}{\text{Slope of the calibration curve}} \quad \text{(eq 3)}$$

$$\text{LOQ} = \frac{10 \times \text{Standard deviation of the intercept}}{\text{Slope of the calibration curve}} \quad \text{(eq 4)}$$

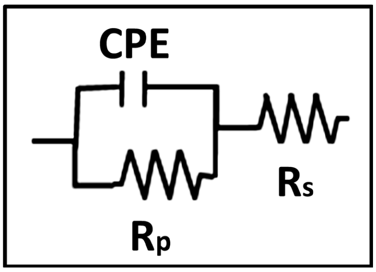

Figure 4. Model equivalent electrical circuit (EEc) of the Pt/oligomer/electrolyte interface and its: Rs is the solution and contact resistance, Rp is the polarization resistance of the polymer film, CPE is the constant phase elements of the polymer film/electrolyte interface.

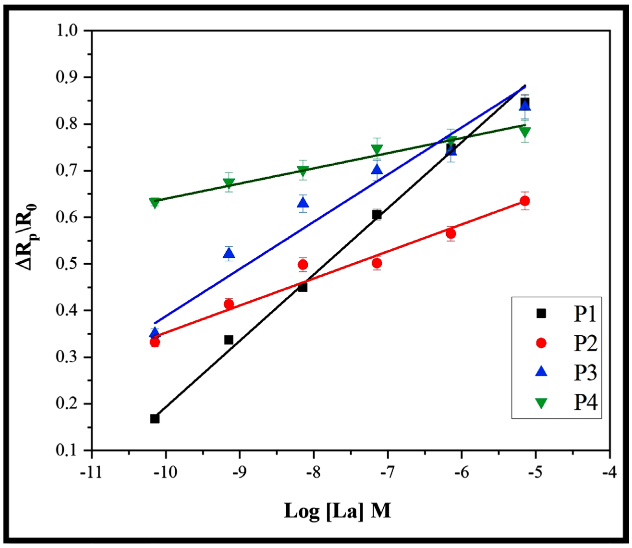

Figure 5. Relative variation of the polarization resistance of the oligomer-modified platinum electrode/electrolyte interface as a function of log concentration of La ion (M).

As shown in **Table 3**, the OH-oligo(ether-sulfone) (P1), presents a higher sensitivity value. The presence of the dihydroxyl groups at the end of P1 chains improves the hydrophilic properties of the polymer. Lanthanum ions present six coordination links with oxygen atoms of the isosorbide group, and the sulfone group as designed for 2-MNBBSH-Yterbium-complex (**Figure 6**). Other trivalent ions were tested in this work and presented lower affinity for the 2-MNBBSH than the REE, Y^{3+}, even at a 10 times higher concentration [29].

Table 3. Detection limits, quantification limits, linear range, and sensitivities obtained for La ions.

Sensing polymers	Sensitivity	LOD [M]	LOQ [M]	Linear range [M]
P1	0.142	1×10^{-9}	3.33×10^{-9}	10^{-10} - 10^{-5}
P2	0.058	5×10^{-9}	1.66×10^{-8}	10^{-10} - 10^{-5}
P3	0.111	3×10^{-9}	1×10^{-8}	10^{-10} - 10^{-5}
P4	0.032	6×10^{-9}	2×10^{-8}	10^{-10} - 10^{-5}

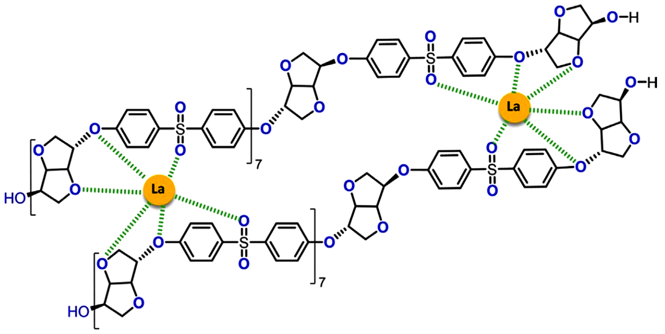

Figure 6. Hydrophilic interactions of La ion with P1 oligo (ether sulfone).

The analytical performance of this impedimetric sensor for La detection was compared to that of previously published electrochemical sensors in **Table 4**. A very low detection limit is obtained with EIS, compared to those obtained with potentiometric and voltammetric La sensors.

Table 4. Comparison of the analytical performance of the La impedimetric sensor to that of previously published electrochemical sensors.

REE	Electrode	Method	Detection Limit	Dynamic range	Ref
La	PVC membrane including BNOPC + CCD	potentiometry	5×10^{-7} M Sensitivity 26 mV/dec.	10^{-5} M - 10^{-3} M	[30]
La	Tin electrode Alizarin complexon	Adsorptive Stripping Voltammetry	0.42 µg/L	1 - 25 µg/L	[31]
La	Oligo (ether sulfone)s	EIS	10^{-9} M	10^{-9} M - 10^{-5} M	This work

3.4. EIS Measurements for Detecting Ce

The obtained Nyquist plots in the complex plane are shown in **Figure 7**. A significant decrease in impedance was observed after increasing cerium concentration. This observation confirms that the polarization resistance of the polymer/electrolyte interface decreases. This is attributed to chemical bonds between Ce ions and the oligo (ether sulfone) as described for La ions.

Calibration curves were obtained by plotting the relative variation of the polarization resistance as a function of Ce concentrations (**Figure 8**). The relative change ($\Delta R/R$) of the oligo (ether sulfone)s P1 - P4 modified electrodes is linearly proportional to the logarithmic value of Ce concentration. The detection sensitivity is defined as the slope of the $\Delta R/R$ calibration curves as a function of the logarithm of Ce concentration. **Table 5** gathers the results obtained with the different oligo (ether sulfone)s, showing that the P1 oligomer presents a higher sensitivity. Due to hydrophilic properties, the presence of dihydroxyl groups in the structure of oligomer P1 improves the adsorption efficiency of Ce ions. The relative standard deviation on the relative variation of the polarization resistance is 5%. The repeatability between the three P1-based sensors was 10%.

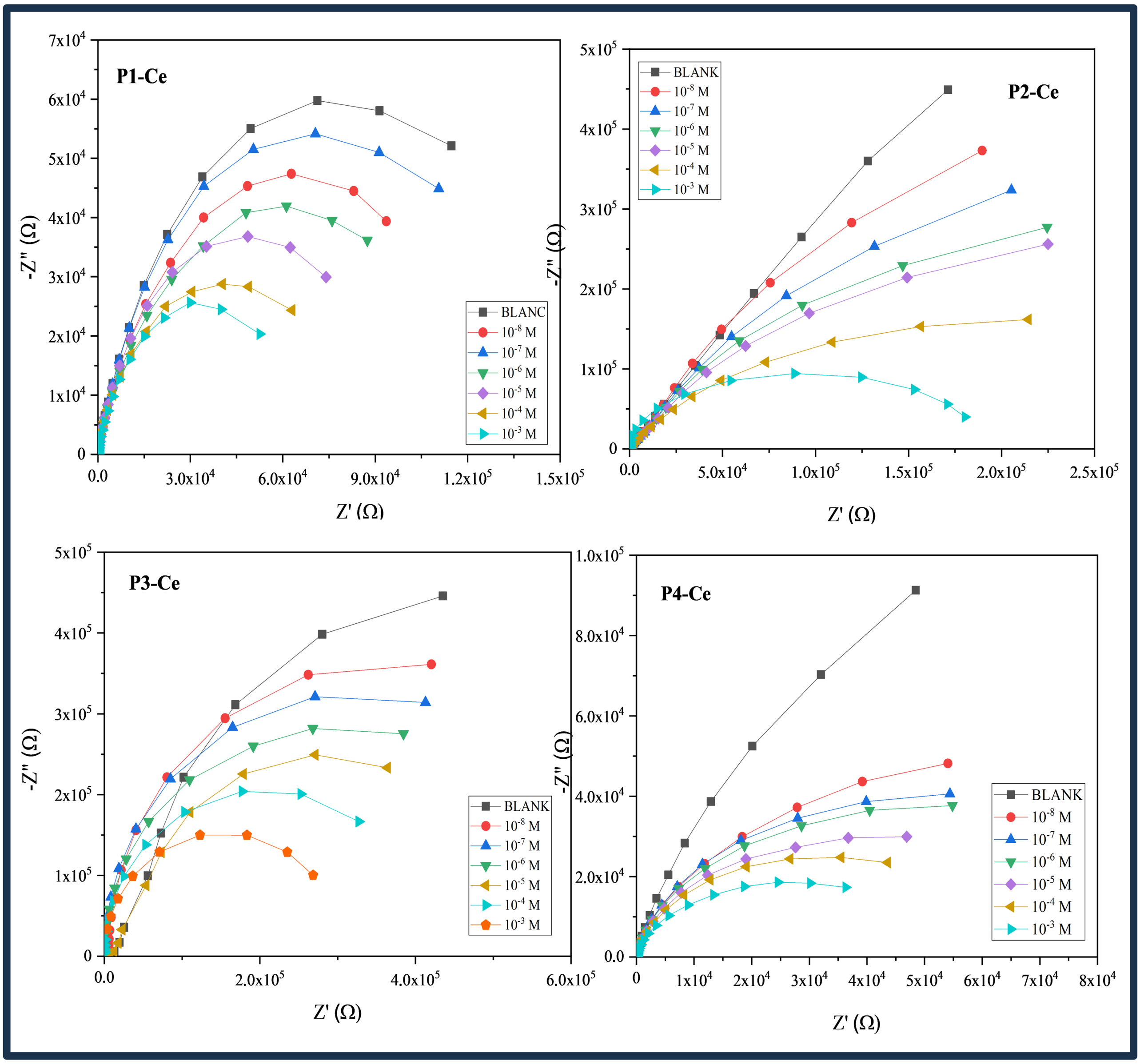

Figure 7. Nyquist plots of Pt/oligomer/electrolyte interface obtained in the presence of Ce ions.

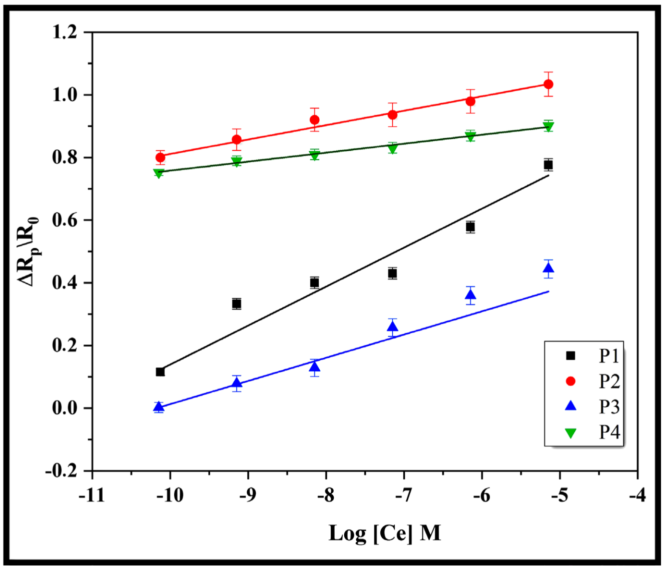

Figure 8. Relative variation of the polarization resistance of the oligomer-modified platinum electrode/electrolyte interface as a function of log concentration of La ion (M).

Table 5. Comparative study: of the responses of sensors based on oligomers P1, P2, P3, and P4 for Ce detection.

Sensing polymers	Sensitivity	LOD [M]	LOQ [M]	Linear range [M]
P1	0.124	3×10^{-9}	1×10^{-8}	10^{-10} - 10^{-5}
P2	0.046	8×10^{-9}	2.7×10^{-8}	10^{-10} - 10^{-5}
P3	0.078	3×10^{-9}	1×10^{-8}	10^{-10} - 10^{-5}
P4	0.029	1×10^{-9}	3.3×10^{-9}	10^{-10} - 10^{-5}

The analytical performance of this impedimetric sensor for Ce detection was compared to that of previously published electrochemical sensors in Table 6. A very low detection limit is obtained with EIS, compared to those obtained with voltammetric Ce sensors, except in [31] when an ion-imprinted polymer was used.

Table 6. Comparison of the analytical performance of the Ce impedimetric sensor to that of previously published electrochemical sensors.

REE	Electrode	Method	Detection Limit	Dynamic range	Ref
Ce	Tin electrode Alizarin complexon	Adsorptive Stripping Voltammetry	0.06 μg/L	1 - 25 μg/L	[31]
Ce	Ce(III)-IIM/PC/GCE	Stripping voltammetry	10^{-12} M	3.0×10^{-12} - 1.0×10^{-4} M	[32]
Ce	Ce(III)-IIM/CPE	Stripping voltammetry	1.5×10^{-7} M	10^{-5} - 2.0×10^{-4} M	[33]
Ce	DAN-GQDs GNB-modified-CF electrode	CV DPV	2.60 μM		[34]
Ce	Oligo (ether sulfone)s	EIS	3×10^{-9} M	10^{-9}M - 10^{-5} M	This work

4. Conclusion

In this work, we developed a novel electrochemical sensor using an oligo (ether sulfone)-modified platinum electrode for the sensitive detection of rare earth elements, in particular the most abundant in the earth's crust, lanthanum (La) and cerium (Ce). Electrochemical impedance spectroscopy (EIS) was used for detecting La and Ce ions over a wide concentration range from 10^{-9} M to 10^{-5} M, reaching a low detection limit of 10^{-9} M and 3×10^{-9} M respectively. The electrochemical sensor, composed of dihydroxy-oligo (ether sulfone) (P1), demonstrated significantly higher sensitivity for La and Ce ions and low detection limits compared to other oligo (ether sulfone)s with difluorinated, diamine and bismaleimide end groups. This obtained sensor presents a lower detection limit, compared to most of the published electrochemical sensors. Further studies involving characterization techniques will be carried out to provide evidence of polymer-REE interactions. The application of this simple sensor for the detection of REE in real samples should be validated by comparing the results with those of the classical analytical techniques.

Acknowledgments

The authors would like to acknowledge the financial support of the POLYAM project, of the High Ministry of Education and Research in Tunisia. CNRS is acknowledged for the IRP NARES.

Conflicts of Interest

The authors declare no conflicts of interest regarding the publication of this paper.

References

[1] BRGM (2022) Les Terres Rares. Dossier "Enjeux des Géosciences". https://www.brgm.fr

[2] European Commission: Directorate-General for Internal Market, Industry, Entrepreneurship and SMEs, Grohol, M. and Veeh, C. (2023) Study on the Critical Raw Materials for the EU 2023. https://data.europa.eu/doi/10.2873/725585

[3] Ali, S. (2014) Social and Environmental Impact of the Rare Earth Industries. *Resources*, **3**, 123-134. https://doi.org/10.3390/resources3010123

[4] Zapp, P., Schreiber, A., Marx, J. and Kuckshinrichs, W. (2022) Environmental Impacts of Rare Earth Production. *MRS Bulletin*, **47**, 267-275. https://doi.org/10.1557/s43577-022-00286-6

[5] Sitko, R., Janik, P., Zawisza, B., Talik, E., Margui, E. and Queralt, I. (2015) Green Approach for Ultratrace Determination of Divalent Metal Ions and Arsenic Species Using Total-Reflection X-Ray Fluorescence Spectrometry and Mercapto-Modified Graphene Oxide Nanosheets as a Novel Adsorbent. *Analytical Chemistry*, **87**, 3535-3542. https://doi.org/10.1021/acs.analchem.5b00283

[6] Borai, E., Ekhlom, P. and Harjula, R. (2014) Group Separation of Heavy Metals Followed by Subsequent and Individual Separation of Lanthanides by Chelation

Chromatography. *Journal of Liquid Chromatography & Related Technologies*, **37**, 1614-1631. https://doi.org/10.1080/10826076.2013.803204

[7] He, M., Hu, B. and Jiang, Z. (2005) Electrothermal Vaporization Inductively Coupled Plasma Mass Spectrometry for the Determination of Trace Amount of Lanthanides and Yttrium in Soil with Polytetrafluroethylene Emulsion as a Chemical Modifier. *Analytica Chimica Acta*, **530**, 105-112. https://doi.org/10.1016/j.aca.2004.08.074

[8] Buseth, E., Wibetoe, G. and Martinsen, I. (1998) Determination of Endogenous Concentrations of the Lanthanides in Body Fluids and Tissues Using Electrothermal Vaporization Inductively Coupled Plasma Mass Spectrometry. *Journal of Analytical Atomic Spectrometry*, **13**, 1039-1049. https://doi.org/10.1039/a801612g

[9] Cao, X.D., Yin, M., Wang, X.R. and Zhao, G.W. (1999) Determination of Trace Rare Earth Elements in Soils by Inductively Coupled Plasma-Mass Spectrometry after Microwave Digestion for Sample Preparation. *Chinese Journal of Analytical Chemistry*, **27**, 679-683.

[10] Yelkenci, H.E. and Öztekin, N. (2016) Separation and Sensitive Detection of Lanthanides by Capillary Electrophoresis and Contactless Conductivity Detection. *Journal of Chromatographic Science*, **55**, 465-470. https://doi.org/10.1093/chromsci/bmw200

[11] Hirokawa, T. and Hashimoto, Y. (1997) Simultaneous Separation of Yttrium and Lanthanide Ions by Isotachophoresis. *Journal of Chromatography A*, **772**, 357-367. https://doi.org/10.1016/s0021-9673(97)00055-1

[12] Nukatsuka, I., Taga, M. and Yoshida, H. (1981) Separation of Lanthanides by Capillary Tube Isotachophoresis Using Complex-Forming Equilibria. *Journal of Chromatography A*, **205**, 95-102. https://doi.org/10.1016/s0021-9673(00)81817-8

[13] Hirokawa, T., Xia, W. and Kiso, Y. (1995) Isotachophoretic Separation of Rare Earth Ions I. Separation Behaviour of Yttrium and Fourteen Lanthanide Ions Forming Complexes with Tartaric Acid and A-Hydroxyisobutyric Acid. *Journal of Chromatography A*, **689**, 149-156. https://doi.org/10.1016/0021-9673(94)00872-7

[14] Hirokawa, T., Aoki, N. and Kiso, Y. (1984) Complex-Forming Equilibria in Isotachophoresis. VI. Simulation of Isotachophoretic Equilibria of Lathanoids and Determination Mobilities and Stability Constants of Acetate and β-Hydroxyisobutyrate Complexes. *Journal of Chromatography A*, **312**, 11-29. https://doi.org/10.1016/s0021-9673(01)92760-8

[15] Mao, Q., Hashimoto, Y., Manabe, Y., Ikuta, N., Nishiyama, F. and Hirokawa, T. (1998) Separation of Rare-Earth Ions by Isotachophoresis and Capillary Zone Electrophoresis. *Journal of Chromatography A*, **802**, 203-210. https://doi.org/10.1016/s0021-9673(97)01093-5

[16] Lombard, S.M. and Isenhour, T.L. (1969) Determination of Samarium and Gadolinium in Rare Earth Ores by Neutron-Capture Gamma-Ray Activation Analysis. *Analytical Chemistry*, **41**, 1113-1116. https://doi.org/10.1021/ac60277a039

[17] Paderni, D., Giorgi, L., Fusi, V., Formica, M., Ambrosi, G. and Micheloni, M. (2021) Chemical Sensors for Rare Earth Metal Ions. *Coordination Chemistry Reviews*, **429**, Article ID: 213639. https://doi.org/10.1016/j.ccr.2020.213639

[18] Alenazi, N.A., Alam, M.M., Hussein, M.A., Alamry, K.A., Asiri, A.M. and Rahman, M.M. (2018) Functionalized Polyethersulfone as PES-NH2-Metal Oxide Nanofilers for the Detection of Y^{3+}. *Polymer Bulletin*, **76**, 4485-4506. https://doi.org/10.1007/s00289-018-2612-7

[19] Chatti, S., Kricheldorf, H.R. and Schwarz, G. (2006) Copolycarbonates of Isosorbide and Various Diols. *Journal of Polymer Science Part A*: *Polymer Chemistry*, **44**, 3616-3628. https://doi.org/10.1002/pola.21444

[20] Besse, V., Auvergne, R., Carlotti, S., Boutevin, G., Otazaghine, B., Caillol, S., *et al.* (2013) Synthesis of Isosorbide Based Polyurethanes: An Isocyanate Free Method. *Reactive and Functional Polymers*, **73**, 588-594. https://doi.org/10.1016/j.reactfunctpolym.2013.01.002

[21] Nelson, A.M. and Long, T.E. (2012) A Perspective on Emerging Polymer Technologies for Bisphenol—A Replacement. *Polymer International*, **61**, 1485-1491. https://doi.org/10.1002/pi.4323

[22] Fenouillot, F., Rousseau, A., Colomines, G., Saint-Loup, R. and Pascault, J. (2010) Polymers from Renewable 1,4:3,6-Dianhydrohexitols (Isosorbide, Isomannide and Isoidide): A Review. *Progress in Polymer Science*, **35**, 578-622. https://doi.org/10.1016/j.progpolymsci.2009.10.001

[23] Feng, X., East, A.J., Hammond, W.B., Zhang, Y. and Jaffe, M. (2010) Overview of Advances in Sugar-Based Polymers. *Polymers for Advanced Technologies*, **22**, 139-150. https://doi.org/10.1002/pat.1859

[24] Hale, W.F., Farnham, A.G., Johnson, R.N. and Clendinning, R.A. (1967) Poly(Aryl Ethers) by Nucleophilic Aromatic Substitution. II. Thermal Stability. *Journal of Polymer Science Part A*-1: *Polymer Chemistry*, **5**, 2399-2414. https://doi.org/10.1002/pol.1967.150050917

[25] Rose, J.B. (1974) Synthetic Routes to Poly (Ether Sulfone)s. *Chimia*, **38**, 561-567.

[26] Kricheldorf, H.R. (1992) Handbook of Polymer Syntheses. Marsel Dekker.

[27] Mechichi, R., Chabbah, T., Chatti, S., Jlalia, I., Sanglar, C., Casabianca, H., *et al.* (2022) Semi-Interpenetrating Network-Coated Silica Gel Based on Green Resources for the Efficient Adsorption of Aromatic Pollutants from Waters. *Chemistry Africa*, **5**, 2241-2258. https://doi.org/10.1007/s42250-022-00463-9

[28] Belgacem, C., Medimagh, R., Kricheldorf, H., Ben Romdhane, H. and Chatti, S. (2016) Copolyethersulfones of 1,4:3,6-Dianhydrohexitols and Bisphenol A. *Designed Monomers and Polymers*, **19**, 248-255. https://doi.org/10.1080/15685551.2015.1136531

[29] Hussain, M.M., Rahman, M.M., Arshad, M.N. and Asiri, A.M. (2017) Trivalent Y^{3+} Ionic Sensor Development Based on (e)-Methyl-N'-Nitrobenzylidene-Benzenesulfonohydrazide (MNBBSH) Derivatives Modified with Nafion Matrix. *Scientific Reports*, **7**, Article No. 5832. https://doi.org/10.1038/s41598-017-05703-4

[30] Kirsanov, D.O., Legin, A.V., Babain, V.A. and Vlasov, Y.G. (2005) Polymeric Sensors Based on Extraction Systems for Determination of Rare-Earth Metals. *Russian Journal of Applied Chemistry*, **78**, 568-573. https://doi.org/10.1007/s11167-005-0343-7

[31] Makombe, M., van der Horst, C., Silwana, B., Iwuoha, E. and Somerset, V. (2016) Antimony Film Sensor for Sensitive Rare Earth Metal Analysis in Environmental Samples. *Journal of Environmental Science and Health*, *Part A*, **51**, 597-606. https://doi.org/10.1080/10934529.2016.1159857

[32] Chen, J., Bai, H., Li, Z., Xia, J. and Cao, Q. (2018) Stripping Voltammetric Determination of Cerium in Food Using an Electropolymerized Poly-Catechol and Ion-Imprinted Membrane Modified Electrode. *Journal of Electroanalytical Chemistry*, **808**, 41-49. https://doi.org/10.1016/j.jelechem.2017.11.049

[33] Chen, J., Bai, H., Xia, J., Liu, X., Liu, Y. and Cao, Q. (2018) Trace Detection of Ce^{3+} by Adsorption Strip Voltammetry at a Carbon Paste Electrode Modified with Ion Imprinted Polymers. *Journal of Rare Earths*, **36**, 1121-1126. https://doi.org/10.1016/j.jre.2018.03.014

[34] Ravi, P.V., Thangadurai, D.T., Nehru, K., Lee, Y.I., Nataraj, D., Thomas, S., *et al.* (2020) Surface and Morphology Analyses, and Voltammetry Studies for Electrochemical

Determination of Cerium(III) Using a Graphene Nanobud-Modified-Carbon Felt Electrode in Acidic Buffer Solution (pH 4.0 ± 0.05). *RSC Advances*, **10**, 37409-37418. https://doi.org/10.1039/d0ra07555h